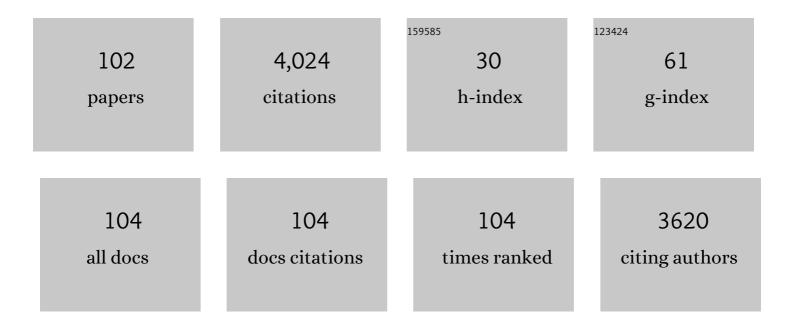
## Paschal Nbelayim

List of Publications by Year in descending order

Source: https://exaly.com/author-pdf/3435878/publications.pdf Version: 2024-02-01



#	Article	IF	CITATIONS
1	Heteroatom doping of 2D graphene materials for electromagnetic interference shielding: a review of recent progress. Critical Reviews in Solid State and Materials Sciences, 2022, 47, 570-619.	12.3	68
2	Synthesis of 3Li2S–1P2S5–xLiI solid electrolytes by liquid-phase shaking method for all-solid-state Li metal batteries. Journal of Sol-Gel Science and Technology, 2022, 101, 16-23.	2.4	5
3	Functionalities and modification of sol–gel derived SiO <sub>2</sub> –TiO <sub>2</sub> systems for advanced coatings and powders. Journal of the Ceramic Society of Japan, 2022, 130, 143-162.	1.1	2
4	Synthesis of an All <sub>3</sub> -doped Li <sub>2</sub> S positive electrode with superior performance in all-solid-state batteries. Materials Advances, 2022, 3, 2488-2494.	5.4	11
5	Li <sub>4</sub> SiO <sub>4</sub> Doped-Li <sub>7</sub> P <sub>2</sub> S <sub>8</sub> I solid electrolytes with high lithium stability synthesised using liquid-phase shaking. RSC Advances, 2022, 12, 7469-7474.	3.6	2
6	Mechanical Properties of Sulfide-Type Solid Electrolytes Analyzed by Indentation Methods. ACS Applied Energy Materials, 2022, 5, 2349-2355.	5.1	19
7	Preparation of Cal <sub>2</sub> -Doped Li <sub>7</sub> P <sub>3</sub> S <sub>11</sub> by Liquid-Phase Synthesis and Its Application in an All-Solid-State Battery with a Graphite Anode. Energy & Fuels, 2022, 36, 4577-4584.	5.1	3
8	Li <sub>7</sub> P <sub>2</sub> S <sub>8</sub> I solid electrolytes synthesized by liquid-phase synthesis with improved heat treatment process. Journal of the Ceramic Society of Japan, 2022, 130, 299-302.	1.1	2
9	An overview of recent progress in nanostructured carbon-based supercapacitor electrodes: From zero to bi-dimensional materials. Carbon, 2022, 193, 298-338.	10.3	168
10	Solution Processing via Dynamic Sulfide Radical Anions for Sulfide Solid Electrolytes. Advanced Energy and Sustainability Research, 2022, 3, .	5.8	8
11	High Ionic Conductivity with Improved Lithium Stability of CaS- and Cal <sub>2</sub> -Doped Li <sub>7</sub> P <sub>3</sub> S <sub>11</sub> Solid Electrolytes Synthesized by Liquid-Phase Synthesis. ACS Omega, 2022, 7, 16561-16567.	3.5	3
12	Fabrication and Electrochemical Characterization of an All-solid-state Battery with an Anti-perovskite Electrode Material (Li2Fe)SO. Chemistry Letters, 2022, 51, 690-692.	1.3	0
13	Ionic Conduction and Electric Modulus in Li <sub>2</sub> S–CaS and Ca <i>X</i> <sub>2</sub> ( <i>X</i> = F, Cl, Br, and I) Nanocomposites. Electrochemistry, 2022, 90, 067005-067005.	1.4	4
14	<i>In situ</i> growth of laser-induced graphene micro-patterns on arbitrary substrates. Nanoscale, 2022, 14, 8914-8918.	5.6	44
15	Nanomaterial Fabrication through the Modification of Sol–Gel Derived Coatings. Nanomaterials, 2021, 11, 181.	4.1	36
16	Effects of Substituting S with Cl on the Structural and Electrochemical Characteristics of Na <sub>3</sub> SbS <sub>4</sub> Solid Electrolytes. ACS Applied Energy Materials, 2021, 4, 6125-6134.	5.1	28
17	Electrostatically assembled SiC–Al2O3 composite particles for direct selective laser sintering. Advanced Powder Technology, 2021, 32, 2074-2084.	4.1	8
18	Structural, Thermal and Electrochemical studies of Sm substituted CrFeO3 Nanoâ€Pervoskites. Journal of Alloys and Compounds, 2021, 870, 159420.	5.5	5

#	Article	IF	CITATIONS
19	An Electrospun Nanofibrous Sensor Based on a Porous (Cr/Zn) Slats Oxide for Voltammetric Detection of Ezetimibe Drug in Real Samples. Electroanalysis, 2021, 33, 2128.	2.9	0
20	The effect of solvent on reactivity of the Li2S–P2S5 system in liquid-phase synthesis of Li7P3S11 solid electrolyte. Scientific Reports, 2021, 11, 21097.	3.3	15
21	Microwave-assisted synthesis of Mn3O4-Fe2O3/Fe3O4@rGO ternary hybrids and electrochemical performance for supercapacitor electrode. Diamond and Related Materials, 2020, 101, 107622.	3.9	102
22	Synthesis of Sulfide Solid Electrolytes through the Liquid Phase: Optimization of the Preparation Conditions. ACS Omega, 2020, 5, 26287-26294.	3.5	22
23	One-pot synthesis of reduced graphene oxide nanosheets anchored ZnO nanoparticles via microwave approach for electrochemical performance as supercapacitor electrode. Journal of Materials Science: Materials in Electronics, 2020, 31, 15456-15465.	2.2	47
24	Effect of annealing temperature on the performance of ZnO thin film-based dye sensitized solar cell. AIP Conference Proceedings, 2020, , .	0.4	4
25	Development and Characterization of Clay–Nanocomposites for Water Purification. Materials, 2020, 13, 3793.	2.9	9
26	Formation of Feâ€embedded graphitic carbon network composites as anode materials for rechargeable Feâ€air batteries. Energy Storage, 2020, 2, e196.	4.3	4
27	Heteroatom doped graphene engineering for energy storage and conversion. Materials Today, 2020, 39, 47-65.	14.2	400
28	Honeycomb-like open-edged reduced-graphene-oxide-enclosed transition metal oxides (NiO/Co3O4) as improved electrode materials for high-performance supercapacitor. Journal of Energy Storage, 2020, 30, 101539.	8.1	112
29	High ionic conductivity of multivalent cation doped Li <sub>6</sub> PS <sub>5</sub> Cl solid electrolytes synthesized by mechanical milling. RSC Advances, 2020, 10, 22304-22310.	3.6	20
30	Development and fabrication of highly flexible, stretchable, and sensitive strain sensor for long durability based on silver nanoparticles–polydimethylsiloxane composite. Journal of Materials Science: Materials in Electronics, 2020, 31, 11897-11910.	2.2	21
31	Green fabrication of 3D hierarchical blossom-like hybrid of peeled montmorillonite-ZnO for in-vitro electrochemical sensing of diltiazem hydrochloride drug. Materials Science and Engineering C, 2020, 111, 110773.	7.3	16
32	Sulfur–Carbon Nano Fiber Composite Solid Electrolyte for All-Solid-State Li–S Batteries. ACS Applied Energy Materials, 2020, 3, 1569-1573.	5.1	29
33	Preparation and Characterization of Stable and Active Pt@TiO <sub>2</sub> Core–Shell Nanoparticles as Electrocatalyst for Application in PEMFCs. ACS Applied Energy Materials, 2020, 3, 3269-3281.	5.1	15
34	Superior performance of Ni(OH)2-ErGO@ NF electrode materials as pseudocapacitance using electrochemical deposition via two simple successive steps. Journal of Energy Storage, 2020, 30, 101485.	8.1	49
35	Design of Heat-Conductive hBN–PMMA Composites by Electrostatic Nano-Assembly. Nanomaterials, 2020, 10, 134.	4.1	12
36	A review on synthesis of graphene, h-BN and MoS2 for energy storage applications: Recent progress and perspectives. Nano Research, 2019, 12, 2655-2694.	10.4	283

#	Article	IF	CITATIONS
37	Nanotube array-based barium titanate–cobalt ferrite composite film for affordable magnetoelectric multiferroics. Journal of Materials Chemistry C, 2019, 7, 10066-10072.	5.5	19
38	PMMA-ITO Composite Formation via Electrostatic Assembly Method for Infra-Red Filtering. Nanomaterials, 2019, 9, 886.	4.1	20
39	Facile formation of Fe3O4-particles decorated carbon paper and its application for all-solid-state rechargeable Fe-air battery. Applied Surface Science, 2019, 486, 257-264.	6.1	17
40	Rapid Nucleation of Reduced Graphene Oxide-Supported Palladium Electrocatalysts for Methanol Oxidation Reaction. Journal of Nanoscience and Nanotechnology, 2019, 19, 7236-7243.	0.9	3
41	Fabrication of an all-solid-state Zn-air battery using electroplated Zn on carbon paper and KOH-ZrO2 solid electrolyte. Applied Surface Science, 2019, 487, 343-348.	6.1	21
42	Facile in-situ simultaneous electrochemical reduction and deposition of reduced graphene oxide embedded palladium nanoparticles as high performance electrode materials for supercapacitor with excellent rate capability. Electrochimica Acta, 2019, 314, 124-134.	5.2	93
43	Facile and fast microwave-assisted formation of reduced graphene oxide-wrapped manganese cobaltite ternary hybrids as improved supercapacitor electrode material. Applied Surface Science, 2019, 481, 296-306.	6.1	86
44	Mechanisms of removal of heavy metal ions by ZnO particles. Heliyon, 2019, 5, e01440.	3.2	131
45	Anhydrous proton conductive xCHS-(1-x)WSiA composites prepared via liquid-phase shaking. Solid State Ionics, 2019, 337, 1-6.	2.7	3
46	Investigation of the anchor layer formation on different substrates and its feasibility for optical properties control by aerosol deposition. Applied Surface Science, 2019, 483, 212-218.	6.1	13
47	Preparation of Li7P2S8I Solid Electrolyte and Its Application in All-Solid-State Lithium-Ion Batteries with Graphite Anode. Electronic Materials Letters, 2019, 15, 409-414.	2.2	31
48	Liquid-phase syntheses of sulfide electrolytes for all-solid-state lithium battery. Nature Reviews Chemistry, 2019, 3, 189-198.	30.2	238
49	Micro- and Nano-assembly of Composite Particles by Electrostatic Adsorption. Nanoscale Research Letters, 2019, 14, 297.	5.7	25
50	Effects of drying temperature on tomato-based thin film as self-powered UV photodetector. Applied Surface Science, 2018, 445, 186-196.	6.1	8
51	Effect of metal/metal oxide coupling on the photoluminescence properties of ZnO microrods. Applied Physics A: Materials Science and Processing, 2018, 124, 1.	2.3	9
52	Sol-gel template synthesis of BaTiO3 films with nano-periodic structures. Materials Letters, 2018, 227, 120-123.	2.6	7
53	Multiferroic nanocomposite fabrication via liquid phase using anodic alumina template. Science and Technology of Advanced Materials, 2018, 19, 535-542.	6.1	5
54	Ag@TiO <sub>2</sub> Nanowires-Loaded Dye-Sensitized Solar Cells and Their Effect on the Various Performance Parameters of DSSCs. Journal of the Electrochemical Society, 2018, 165, H500-H509.	2.9	7

#	Article	IF	CITATIONS
55	Synthesis of plate-like Li3PS4 solid electrolyte via liquid-phase shaking for all-solid-state lithium batteries. Ionics, 2017, 23, 2061-2067.	2.4	96
56	Filamentary Conduction in Aloe Vera Film for Memory Application. Procedia Engineering, 2017, 184, 655-662.	1.2	24
57	Preparation of thermally and chemically robust superhydrophobic coating from liquid phase deposition and low voltage reversible electrowetting. Thin Solid Films, 2017, 636, 273-282.	1.8	12
58	Characterizations and photoelectrochemical properties of Fe2O3 and ZrO2 nanotubes formed by anodic oxidation process. AIP Conference Proceedings, 2017, , .	0.4	0
59	Fast synthesis of Li <sub>2</sub> S–P <sub>2</sub> S <sub>5</sub> –Lil solid electrolyte precursors. Inorganic Chemistry Frontiers, 2017, 4, 1660-1664.	6.0	36
60	Systematic characterization of the effect of Ag@TiO2 nanoparticles on the performance of plasmonic dye-sensitized solar cells. Scientific Reports, 2017, 7, 15690.	3.3	54
61	Controlled facile fabrication of plasmonic enhanced Au-decorated ZnO nanowire arrays dye-sensitized solar cells. Materials Today Communications, 2017, 13, 354-358.	1.9	10
62	Effects of Electrode Materials on Charge Conduction Mechanisms of Memory Device Based on Natural Aloe Vera. MRS Advances, 2016, 1, 2513-2518.	0.9	20
63	Preparation of Li <sub>3</sub> PS <sub>4</sub> Solid Electrolyte by Liquid-Phase Shaking Using Organic Solvents with Carbonyl Group as Complex Forming Medium. Funtai Oyobi Fummatsu Yakin/Journal of the Japan Society of Powder and Powder Metallurgy, 2016, 63, 976-980.	0.2	15
64	Comparison of electrochemical and microbiological characterization of microbial fuel cells equipped with SPEEK and Nafion membrane electrode assemblies. Journal of Bioscience and Bioengineering, 2016, 122, 322-328.	2.2	25
65	Effects of drying temperature and ethanol concentration on bipolar switching characteristics of natural Aloe vera-based memory devices. Physical Chemistry Chemical Physics, 2015, 17, 26833-26853.	2.8	101
66	Voltammetric analysis of nitroxoline in tablets and human serum using modified carbon paste electrodes incorporating mesoporous carbon or multiwalled carbon nanotubes. RSC Advances, 2015, 5, 56086-56097.	3.6	15
67	Blue-emitting photoluminescence of rod-like and needle-like ZnO nanostructures formed by hot-water treatment of sol–gel derived coatings. Journal of Luminescence, 2015, 158, 44-49.	3.1	14
68	A Wettability Tunable Surface of Nafion <sup>®</sup> with Controlling the Flip-Flop Property by DC Applied Voltage. Key Engineering Materials, 2014, 616, 77-81.	0.4	1
69	Ex situ Raman mapping study of mechanism of cordierite formation from stoichiometric oxide precursors. Journal of the European Ceramic Society, 2014, 34, 1009-1015.	5.7	14
70	Preparation of hydroxide ion conductive KOH-ZrO2 electrolyte for all-solid state iron/air secondary battery. Solid State Ionics, 2014, 262, 188-191.	2.7	9
71	Fuel-free low-temperature self-combustion synthesis and characterization of praseodymium-substituted bismuth titanate ceramics. Journal of the Ceramic Society of Japan, 2012, 120, 58-63.	1.1	2
72	Influence of UV irradiation on mechanical properties and structures of sol–gel-derived vinylsilsesquioxane films. Journal of the Ceramic Society of Japan, 2012, 120, 442-445.	1.1	6

#	Article	IF	CITATIONS
73	Mechanical properties comparison of phenylsilsesquioxane-methylsilsesquioxane hybrid films by indentation. Journal of the Ceramic Society of Japan, 2011, 119, 490-493.	1.1	6
74	Texture development of surface-modified SiC prepared by EPD in a strong magnetic field. Journal of the Ceramic Society of Japan, 2011, 119, 667-671.	1.1	4
75	Estimation of interfacial proton conductivity by effective media approximation for sheet-like composite electrolyte prepared from poly(2-acrylamido-2-methyl-1-propanesulfonic acid)-deposited core-shell particles. Journal of the Ceramic Society of Japan, 2011, 119, 845-849.	1.1	Ο
76	Nanometer Scale Proton Conductivity and Dynamics of CsHSO <sub>4</sub> and H <sub>3</sub> PW <sub>12</sub> O <sub>40</sub> Composites under Non-Humidified Conditions. Chemistry of Materials, 2010, 22, 3418-3425.	6.7	10
77	Formation mechanism of titania nanosheet cryatallites on silica–titania gel films by vibration hot-water treatment. Materials Science and Engineering B: Solid-State Materials for Advanced Technology, 2009, 161, 170-174.	3.5	6
78	Effects of Various Additives during Hot Water Treatment on the Formation of Alumina Thin Films for Superhydrophobic Surfaces. Journal of Adhesion Science and Technology, 2008, 22, 387-394.	2.6	7
79	Fabrication of convex-shaped polybenzylsilsesquioxane micropatterns by the electrophoretic sol–gel deposition process using indium tin oxide substrates with a hydrophobic-hydrophilic-patterned surface. Journal of Sol-Gel Science and Technology, 2007, 43, 85-91.	2.4	5
80	Title is missing!. Journal of Sol-Gel Science and Technology, 2003, 27, 61-69.	2.4	42
81	Phosphosilicate Gels as a Solid State Proton Conductor at Medium Temperature and Low Humidity Journal of the Ceramic Society of Japan, 2002, 110, 131-134.	1.3	22
82	Photocatalytic Micropatterning of Transparent Ethylsilsesquioxaneâ^'Titania Hybrid Films. Chemistry of Materials, 2002, 14, 2693-2700.	6.7	22
83	Preparation of Copolymerized Phenylsilsesquioxane-Benzylsilsesquioxane Particles. Journal of Sol-Gel Science and Technology, 2002, 23, 247-252.	2.4	18
84	Proton Conductive Inorganic-Organic Hybrid Membranes as an Electrolyte for Fuel Cells Prepared from 3-Glycidoxypropyltrimethoxysilane and Orthophosphoric Acid. Electrochemistry, 2002, 70, 998-1000.	1.4	11
85	Effects of Addition of Poly(ethylene glycol) on the Formation of Anatase Nanocrystals in SiO2â^'TiO2Gel Films with Hot Water Treatment. Chemistry of Materials, 2001, 13, 2144-2149.	6.7	46
86	Anatase nanocrystalÂdispersed thin films via sol–gel process with hot water treatment: effects of poly(ethylene glycol) addition on photocatalytic activities of the films. Journal of Materials Chemistry, 2001, 11, 2045-2048.	6.7	51
87	Title is missing!. Journal of Sol-Gel Science and Technology, 2001, 22, 41-46.	2.4	33
88	Title is missing!. Journal of Sol-Gel Science and Technology, 2001, 20, 129-134.	2.4	24
89	Thermal Softening Behavior and Application to Transparent Thick Films of Poly(benzylsilsesquioxane) Particles Prepared by the Sol?Gel Process. Journal of the American Ceramic Society, 2001, 84, 775-780.	3.8	45
90	Influences of Preparation Conditions of Sols on Hardening Behaviors of Silica Gel Films for Micro-Patterning Journal of the Ceramic Society of Japan, 2000, 108, 604-606.	1.3	3

#	Article	IF	CITATIONS
91	Thermal Softening Behavior of Poly(phenylsilsesquioxane) and Poly(benzylsilsesquioxane) Particles Journal of the Ceramic Society of Japan, 2000, 108, 830-835.	1.3	32
92	Proton-Conductive Composites Composed of Phosphoric Acid-Doped Silica Gel and Organic Polymers with Sulfo Groups Journal of the Ceramic Society of Japan, 2000, 108, 45-50.	1.3	6
93	Transparent Anatase Nanocomposite Films by the Sol–Gel Process at Low Temperatures. Journal of the American Ceramic Society, 2000, 83, 229-31.	3.8	150
94	Micropatterning on Methylsilsesquioxane– Phenylsilsesquioxane Thick Films by the Sol–Gel Method. Journal of the American Ceramic Society, 2000, 83, 3211-3213.	3.8	17
95	Formation of Anatase Nanocrystals in Sol-Gel Derived TiO2-SiO2 Thin Films with Hot Water Treatment. Journal of Sol-Gel Science and Technology, 2000, 19, 585-588.	2.4	58
96	Title is missing!. Journal of Sol-Gel Science and Technology, 2000, 17, 61-69.	2.4	33
97	Application of Protonic Acid-Doped Silica Gels to Electric Double-Layer Capacitors. Journal of Sol-Gel Science and Technology, 2000, 19, 581-584.	2.4	3
98	Superhydrophobicâ^'Superhydrophilic Micropatterning on Flowerlike Alumina Coating Film by the Solâ^'Gel Method. Chemistry of Materials, 2000, 12, 590-592.	6.7	453
99	Photoredox behavior of methylviologen doped in silica gel matrices. Journal of Materials Chemistry, 2000, 10, 2765-2768.	6.7	1
100	Formation of TiO2(B) Nanocrystallites in Solâ€Gelâ€Derived SiO2â€TiO2 Film. Journal of the American Ceramic Society, 1999, 82, 3248-3250.	3.8	26
101	Fine Patterning and Characterization of Gel Films Derived from Methyltriethoxysilane and Tetraethoxysilane. Journal of the American Ceramic Society, 1998, 81, 2849-2852.	3.8	64
102	Preparation of Transparent Thick Films by Electrophoretic Solâ€Gel Deposition Using Phenyltriethoxysilaneâ€Derived Particles. Journal of the American Ceramic Society, 1998, 81, 2501-2503.	3.8	58